BEAM THEORY MODELS FOR THIN FILM SEGMENTS COHESIVELY BONDED TO AN ELASTIC HALF SPACE

T. W. SHIELD

Department of Aerospace Engineering and Mechanics, University of Minnesota,
Minneapolis, MN 55455, U.S.A.

and

K. S. KIM

Division of Engineering, Brown University, Providence, RI 02912, U.S.A.

Abstract—A thin film segment bonded to an elastic half space is modelled. Previous works have considered membrane models which only take into account the in-plane stiffness of the film and ignore its bending stiffness. To include bending stiffness, a beam theory is used to model the film. The beam model calculations are compared to results from membrane theory. Membrane theory is found to agree with beam theory for the stiffest films, but the energy release rates (or J-integrals) are very close for all films. However, membrane theory can never give information on the normal stresses at the interface and consequently on the mode mixity of the loading at the film edge (or crack tip). To include yielding of the interface at the ends of the film, a cohesive zone model is employed. This zone is a shear zone, that is, only tangential slip in the zone is allowed with no normal opening. The cohesive zone results could be used for determining the interface strengths if the size of the cohesive zone was measured. It was also found that the sign of the normal stress at the tip of the cohesive zone depends on the length of the zone. The structure is loaded by an applied uniform compressive strain in the substrate which can also represent a thermal mismatch strain. The method of solution is to reduce the differential equations for a beam to integral equations which are then coupled to the singular integral equations for a half space. The standard technique of expansion in orthogonal polynomials is used. All the integrations required are performed analytically. The only numerical procedures are in the solution of a set of linear equations and a root finding procedure to determine the cohesive zone size at a given value of the yield stress.

1. INTRODUCTION

The problem of stiffeners on the surface of a half space is not a new one, however with the growth in the integrated circuits market, interest in the problem has been renewed. Previous work, such as Erdogan and Gupta (1971), Jiang and Kim (1987), Freund and Hu (1988), and Erdogan and Joseph (1990), has focused on the membrane model for the thin film. As will be shown, this model characterizes the shear response of the film quite well in most cases, but it does not provide information on the normal stress between the film and the substrate. For a completely bonded film the shear and normal stresses at the interface are both singular at the ends of the film. If the problem were to be treated exactly in the theory of linear elasticity, the results found would be asymptotically the same as the results given by Adams and Bogy (1976). They treat the problem of a semi-infinite strip bonded to an elastic half space. Asymptotically a finite thickness film is not different from a semi-infinite strip, thus Adams and Bogy's results are expected to apply to the problem at hand for a region around the corner of the film where it is bonded to the half space. The dimensions of this region of agreement are much smaller than the thickness of the film. The exact elasticity results predict stresses at the corners whose singularity depends on the two bi-material constants of Dundurs (1969). The strength of this singularity is usually less than 0.5, which is the strength encountered for cracks in homogeneous materials. For some cases of the material parameters, the strength of the singularity is complex and the singularity has an oscillatory nature. When the strength of the singularity is not 0.5 (or it is complex) the solution of the integral equations becomes tedious and the interpretation of the results in the fracture mechanics sense has not been settled. To avoid these problems we will restrict

our study to the cases where the strength of the singularity is 0.5. In one case this will restrict the Poisson's ratio of the substrate to the value of 0.5.

If we treat the thin film as a membrane, that is a layer that has no bending stiffness and only resists axial extension, then the results obtained must be viewed as a first term in an expansion of the exact solution. This is because the response of the film is only modelled using the first term in an expansion in the thickness of the film. The length scale in the expansion must also be compared to the geometry of the problem and thus the order of the expansion determines how close to the film edge such a model will yield accurate predictions. By taking more terms in this expansion, the model will produce valid results closer to the edge of the film. Since bending effects dominate near the ends of the film, and we are interested in the stresses at the ends of the film to predict failure, we must question the accuracy of membrane theory in these regions. Clearly beam theory is only one more term in the expansion and the results we obtain must still be viewed as being applicable only over distances on the order of the film thickness from the end of the film. The advantage to this reduction in the accuracy of the solution near the ends of the film is the reduction in the complexity of the problem and the elimination of the problems encountered when dealing with the exact elasticity solution.

In this paper we will model a segment of film as a classical elastic beam that is perfectly bonded to an elastic substrate. A schematic of the configuration we are considering is shown in Fig. 1. To include nonlinear effects, a cohesive zone will be introduced at the interface at the ends of the film. This zone will be a shear type cohesive zone, that is, only tangential slip will be allowed. The normal stress will be assumed to be perfectly transmitted across the zone and no vertical separation is permitted. This type of model has been chosen because of the dominance of the shear mode in the behavior of thin films and because a separable failure criterion allows the problem to be treated as an almost linear problem. Coupling through a failure criterion that involves both stresses would make the problem completely nonlinear and intractable with the methods employed here. The use of two separate conditions for the shear and normal stresses will be discussed in Section 8. The formulation is also simplified to the membrane model in Section 7 to allow comparison between the two models.
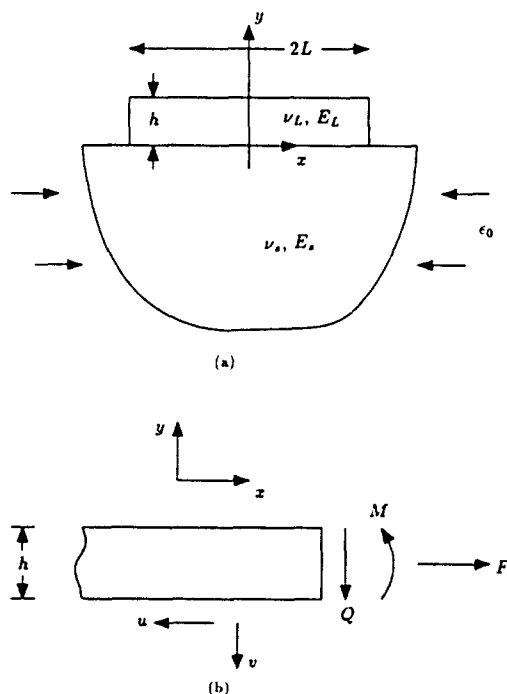

Fig. 1. The geometry of the problem under consideration (a) and the sign conventions used for the beam model (b).

2. THE FILM MODEL

The thin film layer will be modelled as an elastic beam following Shield (1988a). This model will include the membrane model (no bending stiffness) as a special case. Since bending effects are included, it is important to use the bottom surface displacements u and v in the boundary conditions with the surface of the half space.

With the assumption that plane sections remain plane, the vertical displacement at the central line will be v and the horizontal displacement will be $u - h v_x/2$. The subscript x indicates a derivative and h is the layer thickness. The moment, M, and axial force, F, are then given by

$$M = \frac{E_L h^3}{12(1-v_L^2)} v_{xx}, \quad F = \frac{E_L h}{(1-v_L^2)} \left(u_x - \frac{h}{2} v_{xx} \right). \tag{1}$$

where E and v are Young's modulus and Poisson's ratio respectively and the subscripted L indicates layer (film) quantities. The sign conventions are shown in Fig. 1(b). For equilibrium of the layer:

$$\frac{dM}{dx} - Q - \frac{h}{2} q = 0,$$

$$\frac{dQ}{dx} + p = 0, \quad \frac{dF}{dx} - q = 0, \tag{2}$$

where p and q are the normal and shear tractions on the lower surface of the beam and Q is the shear force in the beam. If we differentiate the first of eqns (2) to eliminate Q and use the values (1) for M and F we find that

$$\frac{E_L h^2}{(1-v_L^2)} \left(\frac{1}{2} u_{xxx} - \frac{h}{3} v_{xxxx} \right) - p = 0,$$

$$\frac{E_L h}{(1-v_L^2)} \left(u_{xx} - \frac{h}{2} v_{xxx} \right) - q = 0. \tag{3}$$

Since we wish to approach this problem in terms of integral equations, (3) must be transformed into an integral equation. This amounts to finding the Green's functions for the beam. Since a point load produces a finite displacement at the point of application, the Green's functions are anticipated to be nonsingular. In fact the Green's functions will turn out to be polynomials. In the following let

$$\alpha = \frac{E_L}{1-v_L^2}. \tag{4}$$

The problems we will consider are symmetric with respect to $x = 0$ and the beam extends for $-L \leqslant x \leqslant L$. The ends of the beam are free from tractions. This information will be used in the derivation of the Green's functions. Integrating the first of (3) from 0 to x results in

$$\alpha h \left(\frac{h}{2} u_{xx} - \frac{h^2}{3} v_{xxx} \right) - \int_0^x p(t) \, dt = 0, \tag{5}$$

where the constant of integration has been omitted since it is zero due to the symmetry of the problem. The term u_{xx} can be eliminated from (5) by using the second of (3) to give

$$\frac{\alpha h^3}{12} v_{xxx} + \int_0^x p(t)\,dt - \frac{h}{2}q = 0. \tag{6}$$

Performing another integration gives

$$\frac{\alpha h^3}{12} v_{xx} + \int_0^x p(t)(x-t)\,dt - \frac{h}{2}\int_0^x q(t)\,dt + C_2 = 0. \tag{7}$$

At $x = L$ both the moment M and axial force F are zero. In terms of the lower surface displacements this reduces to $v_{xx}(L) = 0$ and $u_x(L) = 0$. Evaluating (7) at $x = L$ gives

$$C_2 = -\int_0^L p(t)(L-t)\,dt + \frac{h}{2}\int_0^L q(t)\,dt. \tag{8}$$

Equation (7) can be integrated one final time to give

$$\frac{\alpha h^3}{12} v_x + \int_0^x p(t)((x^2+t^2)/2 - xt)\,dt - \frac{h}{2}\int_0^x q(t)(x-t)\,dt + C_2 x = 0. \tag{9}$$

The surface slope vanishes at $x = 0$, thus the constant of integration is zero in (9). Since we are considering a plane strain problem which will be formulated in terms of the x gradients of the surface displacements, this is the required result.

The same procedure for the second of eqns (3) using (6) to eliminate v_{xxx} in favor of u gives

$$u_{xx} - \frac{4}{\alpha h}q + \frac{6}{\alpha h^2}\int_0^x p(t)\,dt = 0. \tag{10}$$

A further integration yields

$$u_x - \frac{4}{\alpha h}\int_0^x q(t)\,dt + \frac{6}{\alpha h^2}\int_0^x p(t)(x-t)\,dt + C_4 = 0, \tag{11}$$

where C_4 is evaluated using the remaining boundary condition at $x = L$, that is, $u_x(L) = 0$. The constant is then found to be

$$C_4 = \frac{4}{\alpha h}\int_0^L q(t)\,dt - \frac{6}{\alpha h^2}\int_0^L p(t)(L-t)\,dt. \tag{12}$$

Equations (9) and (11) can be rearranged and are

$$v_x = \frac{12}{\alpha h^3}\int_0^x p(t)((x^2+t^2)/2 - xt)\,dt - \frac{6}{\alpha h^2}\int_0^x q(t)(x-t)\,dt + \frac{12}{\alpha h^3}C_2 x \tag{13}$$

and

$$u_x = \frac{4}{\alpha h}\int_0^x q(t)\,dt - \frac{6}{\alpha h^2}\int_0^x p(t)(x-t)\,dt - C_4. \tag{14}$$

where C_2 and C_4 are given by (8) and (12). It should be noted that this formulation is only valid for the specific boundary and symmetry conditions used. If other conditions are desired, the derivation above should be repeated. If the problem is not symmetric an

additional unknown, the slope at the center of the beam, is introduced. This unknown would be determined at the same time as the pressure and shear traction distributions.

3. THE HALF SPACE EQUATIONS

The Green's functions for an elastic half space subject to distributed shear and normal tractions are well known [see Johnson (1985) for example] and are

$$(u_s)_x = \frac{2}{\alpha_s \pi} \int_{-L}^{L} \frac{q_s(t)}{t-x} dt - \frac{1-2v_s}{\alpha_s(1-v_s)} p_s(x) - \varepsilon_0 \tag{15}$$

and

$$(v_s)_x = \frac{1-2v_s}{\alpha_s(1-v_s)} q_s(x) + \frac{2}{\alpha_s \pi} \int_{-L}^{L} \frac{p_s(t)}{t-x} dt. \tag{16}$$

where $\alpha_s = E_s/(1-v_s^2)$. The subscript s denotes substrate quantities. The singular integrals must be evaluated in the principal value sense. The loading for this problem is a uniform strain in the half space which is represented by ε_0 in (15). Before proceeding to couple these equations to (13), it is necessary to determine the characteristic behavior of the set of equations we are deriving. The characteristic behavior of a singular integral equation is determined only by the singular terms in the equation [see Muskhelishvili (1953) for example].

The solutions to the equations we are deriving are of the forms

$$p_s(x) = \pi_p(x)(L-x)^\gamma (x+L)^\gamma \tag{17}$$

and

$$q_s(x) = \pi_q(x)(L-x)^\gamma (x+L)^\gamma, \tag{18}$$

where $\pi_p(x)$ and $\pi_q(x)$ are bounded functions of x in $[-L, L]$. Later they will be represented as a sum of orthogonal polynomials, hence the notation. Equations (13) and (14) only involve the integrals of the pressure and the shear, thus if γ is restricted to be greater than -1 these integrals are all bounded at the end points of the interval. The only unbounded terms come from eqns (15) and (16) and they are the only terms that need to be considered in determining the characteristic behavior of the solutions (17) and (18). Following the analysis in Chapter 4 of Muskhelishvili (1953) we find that the exponent γ must satisfy

$$4\cot^2(\pi\gamma) + \frac{(1-2v_s)^2}{(1-v_s)^2} = 0. \tag{19}$$

The general solution to this equation is

$$\gamma = -1/2 + M_\gamma + \frac{\ln(3-4v_s)}{2\pi} i, \tag{20}$$

where M_γ is an integer. A nonzero imaginary part of γ results in an oscillatory solution, which also occurs in the case of an elastic bi-material interface crack. In interface fracture mechanics the imaginary term is called the oscillatory index, ε. Notice that the oscillatory index only depends on the Poisson's ratio of the substrate for this beam analysis. If we wish to consider only solutions that have non-oscillatory behavior at the ends of the film, that is γ real, we must have $v_s = 1/2$, an incompressible substrate. This requirement is removed when cohesive zones at the ends of the film are considered. The negative values of M_γ must

also be ruled out on the physical requirement of bounded total strain energy, that is integrable singularities in p and q.

4. COMPLETELY BONDED CASE

Equations (15) and (16) give the surface displacement gradients of the half space in terms of the applied tractions distributions. Similarly (13) and (14) relate these quantities for the beam. The sign conventions for the two sets of equations are such that for the displacements to be equal we must have

$$u_s = u \quad \text{and} \quad v_s = -v. \tag{21}$$

For the tractions to be equal and opposite in sign requires

$$q_s = q \quad \text{and} \quad p_s = -p. \tag{22}$$

Substituting (15), (16), (13) and (14) into (21) and using (22) results in the following set of equations:

$$0 = \frac{1-2v_s}{(1-v_s)} q(x) - \frac{2}{\pi} \int_{-1}^{1} \frac{p(t)}{t-x} dt - \frac{12}{\beta h^3} \int_{0}^{x} p(t)((x^2+t^2)/2 - xt) dt$$
$$+ \frac{6}{\beta h^2} \int_{0}^{x} q(t)(x-t) dt - \frac{12}{\beta h^3} C_2^* x \tag{23}$$

and

$$-\varepsilon_0 = -\frac{2}{\pi} \int_{1}^{1} \frac{q(t)}{t-x} dt - \frac{1-2v_s}{(1-v_s)} p(x) + \frac{4}{\beta h} \int_{0}^{x} q(t) dt - \frac{6}{\beta h^2} \int_{0}^{x} p(t)(x-t) dt - C_3^* \tag{24}$$

for the tractions on the beam $p(x)$ and $q(x)$. These equations have been nondimensionalized using L as the length scale and α_s as the stress scale. The material constant β (which is not one of the bimaterial constants defined by Dundurs) is given by

$$\beta = \frac{\alpha}{\alpha_s} = \frac{E_L(1-v_s^2)}{E_s(1-v_L^2)}. \tag{25}$$

The film thickness h has been replaced by h/L without a change in notation. The non-dimensional forms of the constants of integration are

$$C_2^* = -\int_{0}^{1} p(t)(1-t) dt + \frac{h}{2} \int_{0}^{1} q(t) dt \tag{26}$$

and

$$C_3^* = \frac{4}{\beta h} \int_{0}^{1} q(t) dt - \frac{6}{\beta h^2} \int_{0}^{1} p(t)(1-t) dt. \tag{27}$$

Since the extent of the bond between the beam and the half space is known in advance, the tractions must be singular at the ends of the beam. Thus the value of M_z in eqn (20) is zero. The polynomials $\pi(x)$ are then chosen to be $T_n(x)$ the Chebyshev polynomials of the first kind because they are orthogonal with respect to the weight function $(1-x^2)^{-1/2}$. The problem is symmetric about $x = 0$ which requires the pressure to be an even function and the shear to be an odd function. Thus, the expansions for the tractions are

$$p(x) = \frac{1}{\sqrt{1-x^2}} \sum_{n=1}^{N} p_n T_{2n}(x) \tag{28}$$

and

$$q(x) = \frac{1}{\sqrt{1-x^2}} \sum_{n=0}^{N} q_n T_{2n+1}(x). \tag{29}$$

Overall equilibrium requires that the resultants of $p(x)$ and $q(x)$ be zero. This is satisfied because the $n = 0$ term in the expansion for $p(x)$ has been omitted and $q(x)$ has been chosen to be an odd function.

Substitution of these expansions into (23) and (24) results in a system of equations:

$$-\varepsilon_0 = \sum_{n=0}^{N} A_n^{11}(x)q_n + \sum_{n=1}^{N} A_n^{12}(x)p_n$$

$$0 = \sum_{n=0}^{N} A_n^{21}(x)q_n + \sum_{n=1}^{N} A_n^{22}(x)p_n, \tag{30}$$

where

$$A_n^{11}(x) = -2U_{2n}(x) + \frac{4}{\beta h}[\Lambda_{2n+1}^0(x) - \Lambda_{2n+1}^0(1)], \tag{31}$$

$$A_n^{12}(x) = -\frac{1-2v_s}{1-v_s} \frac{T_{2n}(x)}{\sqrt{1-x^2}} - \frac{6}{\beta h^2}[x\Lambda_{2n}^0(x) - \Lambda_{2n}^1(x) - \Lambda_{2n}^1(1)], \tag{32}$$

$$A_n^{21}(x) = \frac{1-2v_s}{1-v_s} \frac{T_{2n+1}(x)}{\sqrt{1-x^2}} + \frac{6}{\beta h^2}[x\Lambda_{2n+1}^0(x) - \Lambda_{2n+1}^1(x) - x\Lambda_{2n+1}^0(1)] \tag{33}$$

and

$$A_n^{22}(x) = -2U_{2n-1}(x) - \frac{12}{\beta h^3}\left[\frac{x^2}{2}\Lambda_{2n}^0(x) + \frac{1}{2}\Lambda_{2n}^2(x) - x\Lambda_{2n}^1(x) + x\Lambda_{2n}^1(1)\right]. \tag{34}$$

We have used the integrals given in the Appendix and $\Lambda_{2n}^0(1) = 0$.

These equations involve $2N+1$ unknown coefficients, p_n and q_n, thus we must pick $N+1$ points y_k at which to evaluate eqns (30) in order to find a solution. In Shield (1988b) a variant of the Erdogan and Gupta method (Erdogan et al., 1973) is derived for a similar set of equations and gives the points y_k as

$$y_k = \cos\left(\frac{\pi k}{2N+2}\right). \tag{35}$$

Because the problem we are considering has been formulated as a symmetric problem, only the non-negative values of y_k given by (35) need to be used. There are $N+1$ non-negative values of y_k, but since we have already used the fact that $v_x(0) = 0$, $x = 0$ substituted into the second of (30) gives a trivial equation. Thus, the equations to solve are

$$-\varepsilon_0 = \sum_{n=0}^{N} A_n^{11}(y_k)q_n + \sum_{n=1}^{N} A_n^{12}(y_k)p_n, \quad k = 1, \ldots, N+1$$

$$0 = \sum_{n=0}^{N} A_n^{21}(y_k)q_n + \sum_{n=1}^{N} A_n^{22}(y_k)p_n, \quad k = 1, \ldots, N, \tag{36}$$

which are $2N+1$ equations in $2N+1$ unknowns. These are linear equations in ε_0 thus they only need be solved for one value of this parameter. There are two other parameters that can be varied independently, β, the stiffness ratio and h, the film thickness. The substrate Poisson's ratio is currently restricted to the value of 1 2.

5. OTHER QUANTITIES OF INTEREST

Once the solution for the coefficients in the expansions for the interface tractions has been determined, several other quantities can be calculated. The axial force, F, in the film is related to the interface shear through (2), which can be integrated to give

$$F(x) = \int_0^x q(x)\,dx - \int_0^1 q(x)\,dx,\tag{37}$$

where the boundary condition $F(1) = 0$ has been used. In terms of the expansion (29) this is

$$F(x) = \sum_{n=0}^N q_n[\Lambda_{2n+1}^0(x) - \Lambda_{2n+1}^0(1)].\tag{38}$$

The axial force needed to produce a strain of $-\varepsilon_0$ in the layer is $F_0 = -\varepsilon_0\beta h$. Thus if we divide F in (38) by βh, it takes on the value of -1.0 when the axial strain in the layer is equal to the applied strain in the substrate. The recovery of the axial strain in the layer to the applied strain is of interest for determining the length of film required for buckling to occur at a given loading level.

The relative interface displacements can also be calculated, taking the origin to have zero displacement. Substituting the expansions for the interface tractions into (15) and (16) and then integrating gives:

$$u(x) = 2\sum_{n=0}^N q_n\Gamma_{2n}(x) + \frac{1-2v_s}{1-v_s}\sum_{n=1}^N p_n\Lambda_{2n}^0(x) - \varepsilon_0 x\tag{39}$$

and

$$v(x) = -2\sum_{n=1}^N p_n\Gamma_{2n-1}(x) - \frac{1-2v_s}{1-v_s}\sum_{n=0}^N q_n\Lambda_{2n+1}^0(x),\tag{40}$$

where Γ and Λ are given in the Appendix.

The stress intensity factors for the normal and shear stresses on the interface are

$$K_1(1) = \frac{1}{\sqrt{2}}\sum_{n=1}^N p_n\tag{41}$$

and

$$K_{11}(1) = \frac{1}{\sqrt{2}}\sum_{n=0}^N q_n.\tag{42}$$

These quantities are related to the J-integral of the problem through

$$J = \pi(K_1^2 + K_{11}^2).\tag{43}$$

A mode angle, Φ, can also be defined for this problem to be

$$\Phi = \tan^{-1} \frac{-K_{\text{II}}}{K_{\text{I}}}. \tag{44}$$

This gives an angle of $\pi/2$ for pure shear mode. Note that the mode angle is determined by the materials and the geometry, not the loading, which remains constant for these calculations.

6. INCLUSION OF A SHEAR TYPE COHESIVE ZONE

A simple method of including non-linear effects that occur at the interface is to allow tangential slippage along the interface. That is, we specify a maximum allowable shear stress, τ_y, on the interface. If the shear stress exceeds this value the condition $u_s = u$ is relaxed in that region and replaced by $q = \tau_y$. Examination of the solution to the completely bonded problem formulated above, which is the limit as $\tau_y \to \infty$, shows that the regions where slippage will occur first are near the ends of the beam. In the bonded problem the shear is singular at the ends of the beam. Thus the cohesive zone will be assumed to be

$$|x| \in [a, L], \tag{45}$$

where a is an unknown and must be solved for as part of the solution to the problem. It will only be possible to solve for a if the region (45) is the correct slippage region for the problem. To be consistent the shear stress on the interface must be continuous, that is

$$\lim_{x \to a} q(x) = \tau_y. \tag{46}$$

This will provide an extra equation needed to solve for a.

Nondimensionalizing this problem in the same manner as above, we let $q_y = \tau_y/\alpha$, and a is replaced by a/L. As above we will make this change without a change in notation for a.

In Section 3 it was determined that the Poisson's ratio for the substrate must be equal to $1/2$ for the solution to have non-oscillatory singular behavior at the ends of the beam. This was due to the fact that both of the tractions were singular at the same point. If a shear cohesive zone exists then the shear traction on the interface is bounded and thus the analysis of Section 3 must be altered. The result is that (20) still holds for the exponent in the expansions for p and q but the restriction on v_s is removed. For q to be bounded the choice of M_i is restricted to positive integers, that is, $\gamma = 1/2$ is the smallest value allowable. Terms of the form $(x + L)^\gamma$ can be factored into $(x + L)(x + L)^{\gamma - 1}$. Thus if we change the definition of the bounded function $\pi_q(x)$ to be $(x + L)(L - x)\pi_q(x)$ we can use the expansion (29) for the cohesive zone problem, with the extra condition that the bounded function must have a zero at the points $\pm a$. This is the method described below.

As already explained, the shear traction can be represented by

$$q(x) = \begin{cases} (a^2 - x^2)^{-1/2} \sum_{n=0}^{N} q_n T_{2n+1}(x/a) & |x| \leq a \\ q_y & a \geqslant |x| \geqslant 1 \end{cases}. \tag{47}$$

The integrals from 0 to 1 will have to be broken into two integrals of the form:

$$\int_0^1 q(y)\,dy = \int_0^a q(y)\,dy + q_y(1 - a), \tag{48}$$

where the second integral has been performed. Similarly we find

$$\int_{-1}^{1} \frac{q(y)\,dy}{y-x} = \int_{-a}^{a} \frac{q(y)\,dy}{y-x} + q_v \left[\ln\left(\frac{1-x}{a-x}\right) + \ln\left(\frac{x+a}{x+1}\right) \right] \tag{49}$$

for $|x| \leq a$. The remaining integrals from 0 to x in (24) only need to be evaluated for $|x| \leq a$ because tangential displacement continuity is not enforced in the region $a \geq |x| \geq 1$ where slip is allowed to occur.

Replacing the integrals in (23) and (24) with the appropriate integrals of the form (48) and (49) and using the expansions (28) and (47) we obtain the following set of equations

$$-\varepsilon_0 + q_v B_1(x) = \sum_{n=0}^{N} A_n^{11}(x/a)q_n + \sum_{n=1}^{N} A_n^{12}(x)p_n$$

$$q_v B_2(x) = a \sum_{n=0}^{N} A_n^{21}(x/a)q_n + \sum_{n=1}^{N} A_n^{22}(x)p_n. \tag{50}$$

where

$$A_n^{11}(x/a) = \frac{-2}{a} U_{2n}(x/a) + \frac{4}{\beta h} [\Lambda_{2n+1}^0(x/a) - \Lambda_{2n+1}^0(1)], \tag{51}$$

$$B_1(x) = \frac{4(1-a)}{\beta h} + \frac{2}{\pi} \left[\ln\left(\frac{1-x}{a-x}\right) + \ln\left(\frac{x+a}{x+1}\right) \right], \tag{52}$$

and

$$B_2(x) = \frac{6(1-a)}{\beta h^2} x. \tag{53}$$

The remaining coefficients in (50) are given by (32), (33) and (34). The condition that the bounded part of the expansion for q in (47) has a zero at $\pm a$ is

$$\sum_{n=0}^{N} q_n = 0. \tag{54}$$

This is equivalent to saying that the shear stress intensity factor $K_{11}(a) = 0$.

In this formulation of the cohesive zone problem there are $2N+2$ unknowns: The $2N+1$ coefficients, p_n and q_n and the cohesive zone location a. Equations (50) provide $2N+1$ equations, the first equation is evaluated at $x = ay_k$ for $k = 1,\ldots,N+1$, and the second at $x = y_k$ for $k = 1,\ldots,N$, where y_k is given by (35). Equation (54) provides another equation for a total of $2N+2$. These equations are nonlinear in the cohesive zone location a, thus it is not reasonable to expect a solution to exist for all choices of the parameters ε_0, q_v, β, v, and h. The form of the equations we have derived is $2N+2$ linear equations in the $2N+1$ unknowns p_n and q_n. Thus, these equations will only have a solution if the following condition holds,

$$\det \begin{bmatrix} A^{11} & A^{12} & -\varepsilon_0/q_v + B_1 \\ A^{21} & A^{22} & B_2 \\ 1\cdots 1 & 0\cdots 0 & 0 \end{bmatrix} = 0, \tag{55}$$

where the last row of this matrix represents (54). This equation is of the form:

$$F(a, \varepsilon_0/q_v; \beta, h, v_v) = 0, \tag{56}$$

where the last three parameters will be taken as fixed for the solution of (56). This will

allow solution for a at a given ratio of the loading ε_0 to the shear strength of the interface, q_v. A solution to (56) is found by a suitable root finding algorithm as described in Shield and Bogy (1989). This value is then used in (50) and the coefficients p_n and q_n are found.

The dissipation in the cohesive zone is given by

$$W_p = \int_a^1 \tau_v (u - u_s)_x \, dx \tag{57}$$

which can be reduced to

$$\frac{W_p}{\alpha_s L} = q_v (\Delta u - \Delta u_s), \tag{58}$$

where $\Delta u = u(1) - u(a)$ and similarly for Δu_s. Integrating (15) from a to 1 and using the expansions (28) and (47) gives

$$\Delta u_s = -2 \sum_{n=0}^{N} \frac{q_n}{(2N+1)} (1 - [1/a + (1/a^2 - 1)^{1/2}]^{-(2n+1)}) + \frac{2}{\pi} q_v \left[2a \ln \frac{1+a}{2a} + 2 \ln \frac{1+a}{2} \right]$$
$$- \frac{1-2\nu_s}{1-\nu_s} \sum_{n=1}^{N} p_n \Lambda_{2n}^0(a) - (1-a)\varepsilon_0. \tag{59}$$

Similarly we find

$$\Delta u = \frac{4}{\beta h} \left(a - \frac{a^2+1}{2} \right) q_v + \frac{6}{\beta h^2} \sum_{n=1}^{N} p_n \left[\frac{a^2}{2} \Lambda_{2n}^0(a) - a \Lambda_{2n}^1(a) - \frac{1}{2} (\Lambda_{2n}^2(1) - \Lambda_{2n}^2(a)) + a \Lambda_{2n}^1(1) \right]. \tag{60}$$

The J-integral for the cohesive zone model is

$$J = \pi K_1^2 + \frac{W_p}{\alpha_s L} \tag{61}$$

where K_1 is given by (41).

7. MEMBRANE APPROXIMATION

For comparison between beam and membrane models for a thin film, we will also give the equations for the membrane model here. A membrane can support no normal tractions and provides no resistance to bending. Thus, the relevant equations are (14) and (15) with $p(x) = 0$. This results in the equation

$$-\varepsilon_0 = \sum_{n=0}^{N} q_n \left[-2U_{2n}(x) + \frac{4}{\beta h} (\Lambda_{2n+1}^0(x) - \Lambda_{2n+1}^0(1)) \right], \tag{62}$$

which is evaluated at $x = y_k$ for $k = 1, \ldots, N+1$ to give $N+1$ equations in the $N+1$ unknowns q_n. In this model the material parameters enter the problem only through the single constant βh. The J-integral for the membrane model is

$$J = \pi K_v^2, \tag{63}$$

where K_v is given by K_{11} of (42). The membrane simplification results in a loss of the phase angle information, Φ, which is always $\pi/2$ for this model.

8. RESULTS

The quantities we have described above will be determined for several cases of the material and geometrical parameters that describe the problem. The completely bonded problem is restricted to a substrate of Poisson's ratio of 1 2. To allow comparison, all the other calculations will be done for $v_s = 1$ 2 as well. We will examine cases of the film thickness to half length ratio h of 0.1, 0.05 and 0.01. The relative film stiffness, β, will take the values of 1.0, 10.0 and 100.0. This gives nine combinations to calculate that should display the behaviors of all the quantities adequately. The order of the expansions, N, used is 10 for the bonded solutions and 20 for the cohesive zone model calculations. The cohesive zone calculations will be performed at $a = 0.80$, 0.90, 0.95, 0.98 and 0.99. The loading for both models is represented by the applied strain to the half space ε_0. In all the calculations ε_0 can be taken to be 1.0 without loss in generality because the problems are linear in the applied strain. In the cohesive zone model the size of the zone depends on q_c for a unit applied strain and in general depends on the ratio of τ_s to $\varepsilon_0 \chi_s$ or q_c/ε_0.

The interface stresses p and q are presented in Fig. 2 to show the effect of changing the modulus ratio. Similar trends are seen at the other film thicknesses. The thicker lines are the shear stress, q, and the thinner lines the pressure p. The pressure is positive in the central portion of the film and becomes negative near the end. Negative pressure is tension across the interface, thus not only is the shear stress the largest at the ends of the film but the interface is also in tension. As the layer gets thinner the region where the pressure is non-zero becomes smaller and more localized near the ends of the film. The effects of the bending stiffness of the beam are seen only near the ends. All of the pressure curves go to $-\infty$ as $x \to 1$. The bending effects are also largest for the more compliant films. Figure 3 compares the results of the beam theory calculations with those of membrane theory. A large difference in the shear stress occurs for the more compliant case near the ends of the film. Away from the ends both theories predict similar values of the shear stress.

The axial force in the film is of interest if the possibility of buckling of the film is considered [as in Shield et al. (1991) for example]. Figure 4 gives the axial force for a fixed value of the modulus ratio. Instead of using L as the length scale the results have been rescaled so that h is the length scale. This switch allows the results to be presented as if h were fixed and L varied. This figure shows that the longer the film the higher the axial force in the center of the film and the larger the region where the axial force is large. This allows the length needed for buckling to occur at the center to be calculated. The more compliant the film the faster the axial force in the film increases and the closer it gets to a value of -1.0, which corresponds to the value necessary for the film to have an axial strain of $-\varepsilon_0$.

Figure 5 gives the stress intensity factors K_I and K_{II} versus the film thickness. The shear stress intensity is positive and the normal or mode I intensity is negative. The dashed curves
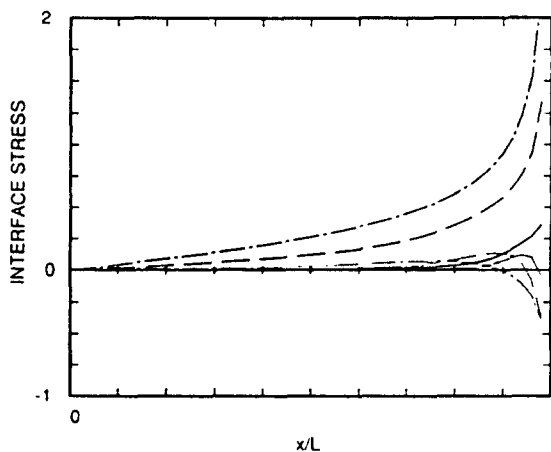

Fig. 2. Beam theory results for the interface shear (thicker curves) and normal (thinner curves) stresses. The film thickness is 0.05 and $\beta = 1.0$ (solid), 10.0 (dashed) and 100.0 (dot-dashed).
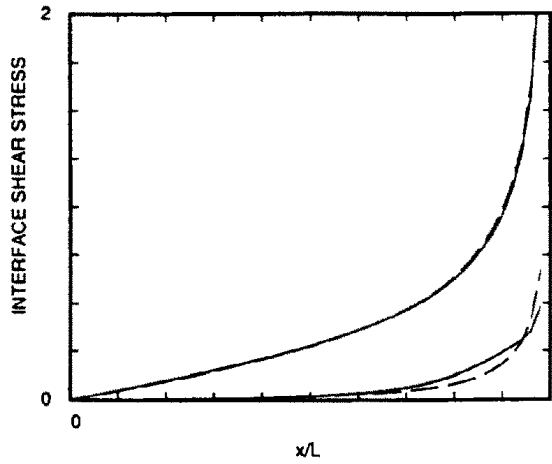
Fig. 3. Comparison of the shear stress predicted by beam (solid) and membrane (dashed) theories for $h = 0.1$ and $\beta = 1.0$ (lower curves) and 100.0 (upper curves).
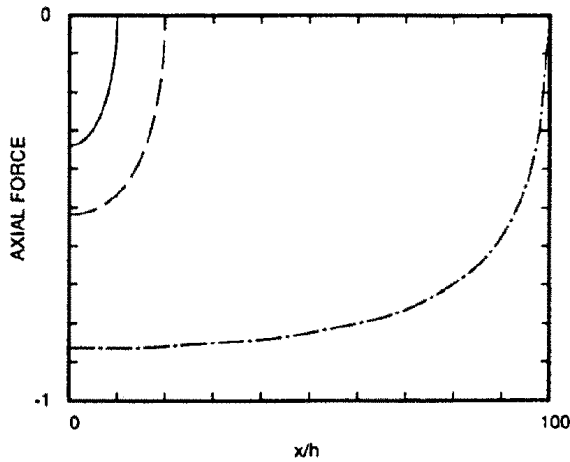

Fig. 4. Beam theory results for the axial force, rescaled to show the effect of changing the length of the film. The modulus ratio is 10.0 and $L/h = 10.0$ (solid), 20.0 (dashed) and 100.0 (dot-dashed).
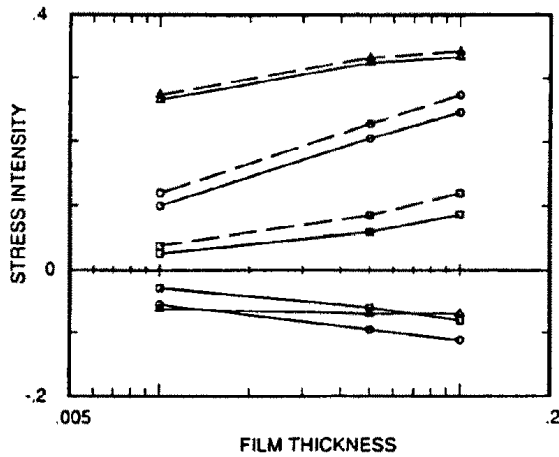

Fig. 5. The stress intensity factors calculated using beam (solid) and membrane (dashed) theories. The modulus ratios are $\beta = 1.0$ (squares), 10.0 (circles) and 100.0 (triangles).
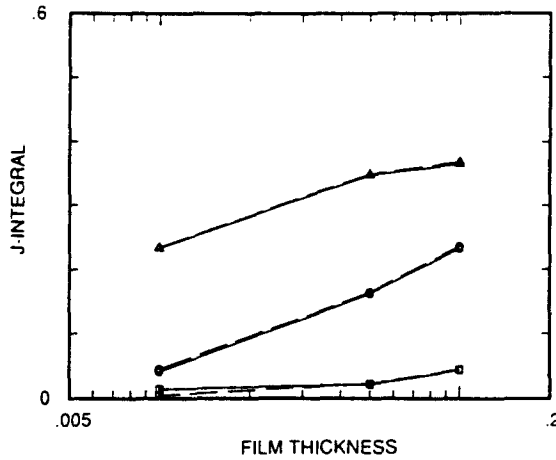
Fig. 6. The J-integral calculated using beam (solid) and membrane (dashed) theories. The modulus ratios are $\beta = 1.0$ (squares), 10.0 (circles) and 100.0 (triangles).

are the results obtained using membrane theory. The J-integrals for the two models are compared in Fig. 6. These results should be identical because the J-integrals away from the film corners are the same and thus the contribution at the corners of the film must match. An important quantity for understanding the behavior of the interface is the mode angle Φ. The mode angle is given in Fig. 7. This figure shows that the mode angle is only weakly dependent on the film thickness and primarily depends on the modulus ratio. The dashed line in Fig. 7 is the result for a semi-infinite film of modulus ratio 1.0 as found by Freund (1990) using the same beam theory model as presented here. This line is an asymptote for the $\beta = 1.0$ curve as the film thickness vanishes. The mode angles for the stiffest films are near $\pi/2$ which is a pure shear mode and the mode angle of the membrane model. The results for $\beta = 1.0$ show nearly equal contributions by the two modes. These results indicate that the membrane model is most reasonable for the stiffest cases where the mode angle is almost $\pi/2$.

The results for the cohesive zone model will be presented for the five values of a given above and four combinations of β and h. These combinations are given in Table 1. Figure 8 presents the zone size, $1-a$, versus the applied stress to yield stress ratio, $1/q_y$, for the various cases under consideration. This has the familiar behavior that zero applied stress produces no yield zone and that the zone size grows with applied stress. Figure 9 shows the interface stresses for two of the material cases and $a = 0.8$. Note that the pressure is positive
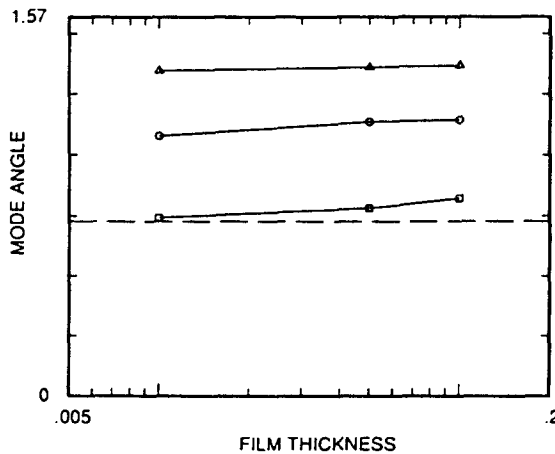

Fig. 7. The mode angle calculated using beam theory. The modulus ratios are $\beta = 1.0$ (squares), 10.0 (circles) and 100.0 (triangles). The dashed line is the result for a semi-infinite film of modulus ratio 1.0.

Table 1. Parameters for the cohesive zone model

Symbol	β	h	βh
Circles	1.0	0.01	0.01
Squares	1.0	0.10	0.10
Inverted triangles	100.0	0.01	1.0
Triangles	100.0	0.10	10.0

at the tip of the cohesive zone and that it still has a negative singularity at the film end. This will be examined in greater detail later. As $a \to 1$ these results approach the results for the completely bonded case.

The pressure is singular at the film end in the cohesive zone model and the variation of K_1 with zone size is given in Fig. 10. The values at a zero zone size are the results from the completely bonded case. A generally smooth approach is made to the completely bonded case results. The curve for the case of $h = 0.1$ and $\beta = 100$, first shows an increase in the magnitude of the normal stress intensity factor but for the largest zone size it is beginning to decrease slightly. The dissipation in the cohesive zone is given in Fig. 11. The greatest dissipation occurs in the stiffest films. The values of the zone dissipation at zero zone size are given by πK_{II}^2, where K_{II} is the shear stress intensity factor from the completely bonded
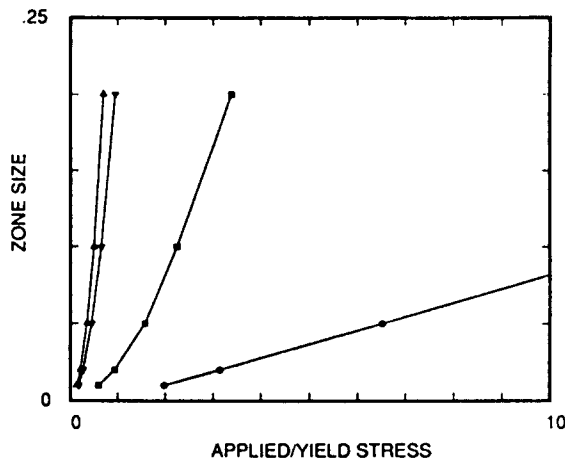

Fig. 8. The zone size versus the applied to yield stress ratio. The film parameters that correspond to the symbols are in Table 1.
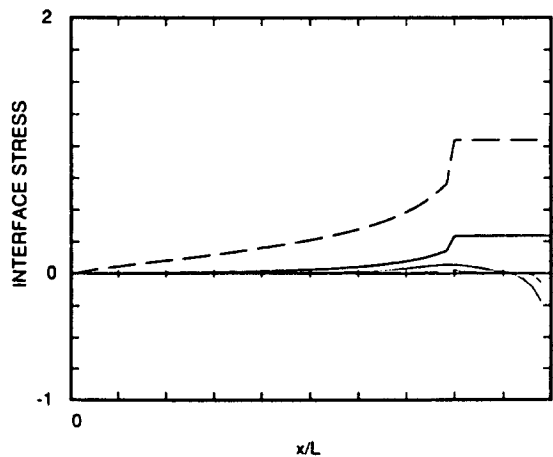

Fig. 9. The interface stresses for a cohesive zone size of 0.2, for film parameters, $h = 0.1$, $\beta = 1.0$ (solid curves) and $h = 0.01$, $\beta = 100.0$ (dashed curves). The thicker curves are the shear stress and the thinner are the normal stress.
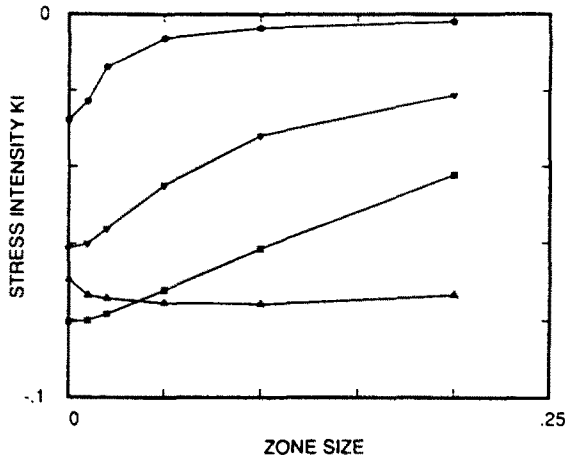
Fig. 10. The normal stress intensity factor versus cohesive zone size. The values at zero zone size are for the completely bonded case. The film parameters that correspond to the symbols are in Table 1.

case. These curves give a validation of the use of the stress intensity factor to characterize the energy released at an infinitesimal zone (crack) tip. Since the pressure is still singular the J-integral of eqn (61) can be used to characterize the complete energy for disbonding at the film edge. This quantity is shown in Fig. 12. This quantity is not constant due to the finite length of the beam, but it is fairly constant for the more compliant cases.

The failure criterion for the cohesive zone model employed here only takes into account the magnitude of the shear stress on the interface. A more complicated model using a yield criterion that also takes into account the normal stress might be postulated as the next step. The use of a yield criterion that involves both the normal and the shear interface stresses would make the problem completely nonlinear and intractable with the approach used here. A separate yield condition for the pressure of the same form as that used for the shear could be incorporated using the same solution techniques as presented here. This would mean that there would be two different (in general) zone sizes. One for the shear yield zone, a as above, and another, b say, for the pressure yield zone. Thus, following a procedure similar to that in Section 6 we would find it necessary to solve two equations of the form of (55) for the two unknowns a and b. This procedure is possible [see Shield and Bogy (1989)] but is very time consuming and has not been attempted for this problem. We can get an idea of the effect of including the pressure in the yield criterion by examining the
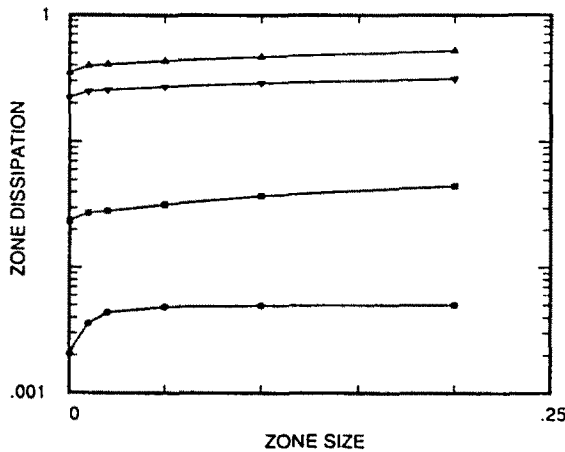

Fig. 11. The dissipation in the cohesive zone versus zone size. The values at zero zone size are πK_{II}^2, where K_{II} is from the completely bonded calculation. The film parameters that correspond to the symbols are in Table 1.
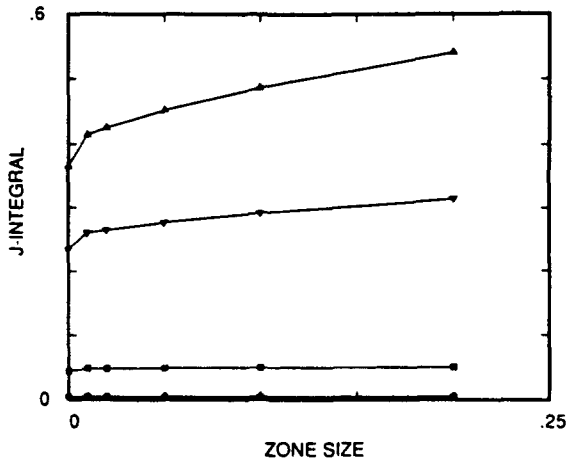
Fig. 12. The J-integral contribution from the cohesive zone versus zone size. The film parameters that correspond to the symbols are in Table 1.

pressure at $x = a$. This is presented in Fig. 13. Note that the pressure generally changes sign from tensile at the zone tip to compressive at some zone size. The curve marked with the solid circles in Fig. 13 only shows positive values of $p(a)$ but it must become negative for some values of the zone size smaller than 0.01 because the pressure in all cases at zero zone size is the completely bonded result of negative infinity. These results indicate that if pressure were included in the yield condition, for small zone sizes there would be an increase in the zone size and above a certain size the zone growth would be retarded by the compressive pressure at the zone tip. As well as considering the pressure at the zone tip, it is of interest to consider the phase angle between the value of the shear (q_v) and the pressure at the tip. These results are given in Fig. 14. Again the values at a zone size of zero are the results from the completely bonded case. The values are all nearly $\pi/2$, which shows that the behavior is dominated by shear in this problem.

9. CONCLUSION

The results presented here allow the limitations of the membrane model of a thin film to be determined. For films with large modulus ratios the membrane model agrees well with the beam model. The lack of normal stress information in the membrane results may affect the ability to predict failures across interfaces that are sensitive to normal stresses. For films
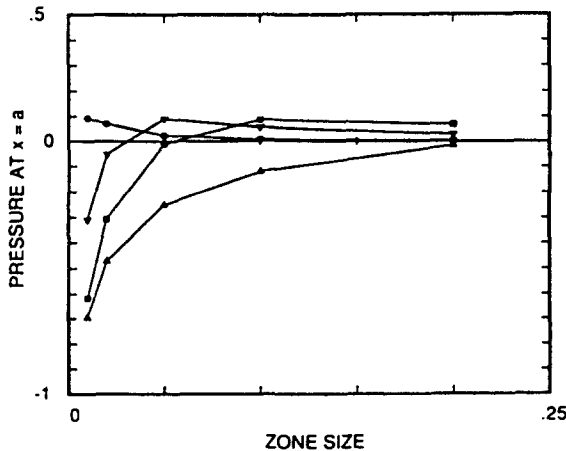

Fig. 13. The pressure at the tip of the cohesive zone, $p(a)$, versus the zone size. The film parameters that correspond to the symbols are in Table 1.
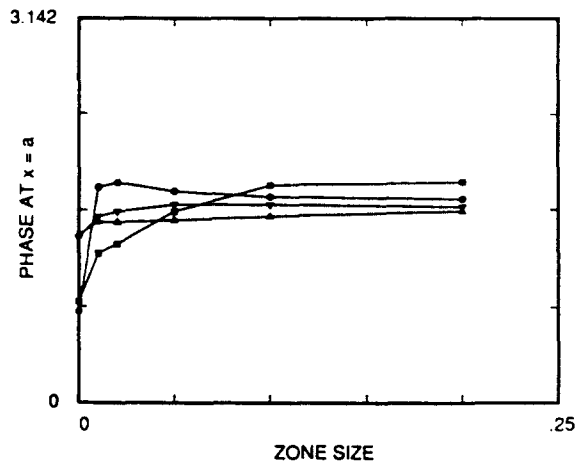
Fig. 14. The mode angle at the tip of the cohesive zone versus zone size. The values at a zone size of zero are from the completely bonded calculation. The film parameters that correspond to the symbols are in Table 1.

whose moduli differ little from the substrate modulus, it is necessary to use at least a beam theory to determine the interface stresses accurately. The cohesive zone results provide a method for determining interfacial strengths if the size of the zone can be measured. The fact that the sign of the normal stress depends on the length of the zone must be taken into account if the interface strength depends on the normal stress. To model an interface whose strength depends largely on the normal stress it may be necessary to employ two cohesive zones. Calculations for two cohesive zones are possible using the analysis presented here, however a full parameter study may be very tedious to complete.

REFERENCES

Abramowitz, M. and Stegun, I. A. (1965). *Handbook of Mathematical Functions*. Dover, New York.
Adams, G. G. and Bogy, D. B. (1976). The plane solution for the elastic contact problem of a semi-infinite strip and half plane. *J. Appl. Mech.* **43**, 603–607.
Dundurs, J. (1969). Discussion. *J. Appl. Mech.* **36**, 650.
Erdogan, F. and Gupta, G. D. (1971). The problem of an elastic stiffener bonded to a half plane. *J. Appl. Mech.* **38**, 937–941.
Erdogan, F., Gupta, G. D. and Cook, T. S. (1973). Numerical solution of singular integral equations. In *Methods of Analysis and Solutions of Crack Problems* (Edited by G. C. Shih), pp. 368–425. Noordhoff, Leyden.
Erdogan, F. and Joseph, P. F. (1990). Mechanical modeling of multilayered films on an elastic substrate, Parts I and II. *J. Electronic Packaging* **112**(4), 309–326.
Freund, L. B. (1990). Private communication.
Freund, L. B. and Hu, Y. (1988). Shear stress at a film-substrate interface due to mismatch strains. Brown University report.
Jiang, W. and Kim, K.-S. (1987). IBM report.
Johnson, K. L. (1985). *Contact Mechanics*. Cambridge University Press, New York.
Muskhelishvili, I. N. (1953). *Singular Integral Equations* (Translated by J. R. M. Radok). Noordhoff, Leyden.
Shield, R. T. (1988a). Private communication.
Shield, T. W. (1988b). Multiple contact region solutions for a flat indenter on a layered elastic half space. Ph.D. Thesis, University of California at Berkeley.
Shield, T. W. and Bogy, D. B. (1989). Multiple region contact solutions for a flat indenter on a layered elastic half space: plane-strain case. *J. Appl. Mech.* **56**(2), 251–262.
Shield, T. W., Kim, K.-S. and Shield, R. T. (1992). The buckling of an elastic layer bonded to an elastic substrate in plane strain. *J. Appl. Mech.* (submitted).

APPENDIX: SOME INTEGRALS OF ORTHOGONAL POLYNOMIALS

Define the symbol $\Lambda_n^m(x)$ as

$$\Lambda_n^m(x) = \int_0^x \frac{y^m T_n(y)}{\sqrt{1-y^2}} \, dy. \tag{A1}$$

where $T_n(y)$ is the Chebyshev polynomial of the first kind. For the case of $m = 0$ Abramowitz and Stegun (1965) in equation 22.13.2 gives:

$$\Lambda_n^0(x) = \begin{cases} \sin^{-1}(x), & n = 0 \\ [U_{n-1}(0) - \sqrt{1-x^2}\,U_{n-1}(x)]/n, & n \geq 1 \end{cases} \tag{A2}$$

where $U_n(x)$ is the Chebyshev polynomial of the second kind. Using integration by parts and other known integrals, the results for the rest of the values of m can be found. For $m = 1$ we found

$$\Lambda_n^1(x) = \begin{cases} 1 - \sqrt{1-x^2}, & n = 0 \\ (\sin^{-1}(x) - x\sqrt{1-x^2})/2, & n = 1 \\ \dfrac{-x}{n}\sqrt{1-x^2}\,U_{n-1}(x) + \dfrac{1}{n}\displaystyle\int_0^x \sqrt{1-y^2}\,U_{n-1}(y)\,dy, & n \geq 2 \end{cases} \tag{A3}$$

where

$$\int_0^x \sqrt{1-y^2}\,U_n(y)\,dy = \frac{1}{n(n+2)}[(n+1)U_{n-1}(0) - \sqrt{1-x^2}\{(n+1)U_{n-1}(x) - nxU_n(x)\}] \tag{A4}$$

is given by Aramowitz and Stegun (1965) in eqn 22.7.21. For $m = 2$ we have

$$\Lambda_n^2(x) = \begin{cases} (\sin^{-1}(x) - x\sqrt{1-x^2})/2, & n = 1 \\ \dfrac{-x^2}{n}\sqrt{1-x^2}\,U_{n-1}(x) + \displaystyle\int_0^x y\sqrt{1-y^2}\,U_{n-1}(y)\,dy, & n \geq 1 \end{cases} \tag{A5}$$

where

$$\int_0^x y\sqrt{1-y^2}\,U_n(y)\,dy = \frac{1}{1 + \dfrac{1}{n+2}}\left\{\frac{x}{n(n+2)}\sqrt{1-x^2}(nxU_n(x) - (n+1)U_{n-1}(x)) + \frac{n+1}{n(n+2)}\int_0^x \sqrt{1-y^2}\,U_{n-1}(y)\,dy\right\} \tag{A6}$$

for $n \geq 1$, and for $n = 0$

$$\int_0^x y\sqrt{1-y^2}\,U_0(y)\,dy = [1 - (1-x^2)^{3/2}]/3. \tag{A7}$$

Another required integral is

$$\Gamma_n(x) = \int_0^x U_n(y)\,dy = \frac{1}{n+1}[T_{n+1}(x) - T_{n+1}(0)]. \tag{A8}$$

The singular integral required is given by Erdogan et al. (1973) eqn (7.96), to be

$$\int_{-1}^1 \frac{T_n(y)\,dy}{(y-x)\sqrt{1-y^2}} = \begin{cases} \pi U_{n-1}(x), & |x| \leq 1 \\ \pi(-1)^{n+1}(x^2-1)^{-1/2}[(x^2-1)^{1/2} - x]^n, & x \geq 1. \end{cases} \tag{A9}$$